



Physics-Informed Neural Network based Probability Density Evolution Method for Reliability Assessment of Self-Centering Viscous Damper

Sourav Das^{1*} and Solomon Tesfamariam²

¹PhD Student, School of Engineering, The University of British Columbia, Okanagan Campus, Kelowna, Canada

²Professor, School of Engineering, The University of British Columbia, Okanagan Campus, Kelowna, Canada

*sds2019@mail.ubc.ca / sourav.das.bony@gmail.com (Corresponding Author)

ABSTRACT

This study presents a reliability-based design optimization (RBDO) method using the probability density evolution method (PDEM) of a steel moment resisting frame coupled with a self-centering viscous damper to estimate the structural design parameters when the structure is subjected to earthquakes. RBDO minimizes the cost function in terms of the probability of failure of the structure in an efficient manner. The PDEM is a well-known reliability analysis method that computes the probability density function of the limit state function by solving a partial differential equation (PDE). The failure probability is estimated by integrating the probability density function of the limit state function over the failure domain. In general, PDEs are solved using the finite difference, finite element, or finite volume methods. RBDO may require many simulations to compute a small failure probability, which leads to computationally expensive solutions for PDEs using traditional methods. In this study, physics-informed neural networks (PINN), a class of machine learning framework, are used to solve the PDE involved in PDEM. PINN is a feedforward neural network that is trained by the physics knowledge involved in PDEs, i.e., the loss function is constructed as a sum of initial, boundary conditions, and state transitions governed by PDEs. In this study, a 16-storey steel moment resisting frame equipped with self-centering viscous dampers at each floor is considered for numerical demonstration. Two types of ensembles of ground motions, i.e., far-field and near-field records, are taken from FEMA P695. The objective of this study is to estimate the design parameters related to a self-centering viscous damper under ground motion uncertainty by minimizing the probability of failure of the maximum inter-storey drift ratio among all floors. The numerical demonstration shows the efficiency of the proposed RBDO framework over the traditional design of the self-centering viscous damper system.

Keywords: Reliability Based Design Optimization, Probability Density Evolution Method, Physics-Informed Neural Network, Deep Learning, Self-Centering Viscous Damper.

INTRODUCTION

In the past decade, reliability-based design optimization (RBDO) has become an open area of research for estimating the structural design parameters when structures are exposed to uncertainties associated with future seismic events. RBDO minimizes the cost function in terms of the probability of failure in an efficient manner. Different methods are used to estimate the probability of failure, such as the analytical approximation method, the numerical sampling-based method, the surrogate-based method, and the numerical integration method. The first-order and second-order reliability methods are common and belong to the analytical approximation method. In these methods, the limit state function is approximated about the most probable point using Taylor's expansion, which leads to inaccurate results when the limit state function is complex or multiple most probable points exist. The numerical sampling-based method includes the Monte Carlo method [1], subset simulation [2], importance sampling [3], etc., which produces more accurate results compared to the analytical approximation method. The main drawback of these methods is their computational cost because they require multiple model evaluations, which can be expensive for complex models or when estimating low failure probabilities. To reduce the computational cost, the surrogate-based methods are one of the alternative solutions that approximates the original limit state function based on a few observations. Kriging [4], polynomial chaos expansion [5], support vector machine [6], artificial neural network [7], etc. are some of the common surrogate models. Despite the advantages of the above-mentioned methods, there are a few limitations to each one. Therefore, the estimation of the probability density function (PDF) of the limit state function is an attractive option

by which the probability of failure is estimated by the PDF of the limit state function over the failure region. This method is known as the numerical integration method. In this study, the numerical integration method is adopted for estimating the probability of failure of the system.

There are different methods available to estimate the PDF of the limit state function, such as the central moments [8], the fractional moments [9], the point estimation method [10], the cubature formulation method [11], etc. The Fokker-Planck-Kolmogorov (FPK) equation is one of the common methods to estimate the transition PDF. Frank et al. [12] used the FPK equation to estimate the transition PDF of the structural response subjected to Gaussian white noise. Due to the complexity of the FPK equation, the applications of this method are limited. However, to overcome this complexity in the solution of the FPK method, the equivalent linearization method [13], the perturbation method [14], and the stochastic averaging method [15] are proposed. The majority of the aforementioned works concentrate on the stationary solution estimated using the FPK equation. The first-passage failure probability must be determined using the transient solution. Because the stationary condition may not be reached before the first passage failure occurs. As the evolution equation is coupled with the physical system in the FPK equation, it is challenging to estimate the transient solution of the FPK equation for a highly nonlinear system with many degrees of freedom.

To overcome this issue, Li and Chen [16] proposed the probability density evolution method (PDEM), in which the principle of probability conservation was used to derive the generalized density evolution method (GDEE) involved in PDEM. The GDEE has an advantage over the FPK equation in that the evolution equation is entirely uncoupled from the physical system. The stochastic response analysis of a 15-storey nonlinear shear building frame under non-stationary ground motion was studied by Xu and Feng [17] using PDEM. For the time-variant reliability assessment of deteriorating structures, Wan et al. [18] proposed an effective PDEM algorithm based on changes in probability measure. By utilising PDEM to evaluate the probabilistic response of the structure, Xu et al. [19] investigated the reliability analysis of the shell structure coupled with a viscoelastic damper. The above studies utilized finite difference method with total variation diminishing (TVD) to solve the GDEE, in which the proper strategy for generating the representative points of random variables present in the system was used so that the representative points should cover the entire domain and PDEM can produce an accurate estimation of PDF. The GF discrepancy-based method [20] is widely used in PDEM to generate the representative points of the random variables. A high number of representative points is necessary for the numerical method of solving the evolution equation in PDEM. As a result, RBDO requires a lot of computational time, which could be inefficient. In this study, a physics-informed neural network (PINN)-based PDEM framework is proposed that not only predicts the PDF but is also used as a solver. PINN is a cutting-edge deep learning technique proposed by Raissi and Karniadakis [21] that forces physical constraints on neural networks. It is a feed-forward neural network in which the loss function is constructed considering the governing physical laws in the form of an ordinary differential equation (ODE) or a partial differential equation (PDE), the initial and boundary conditions of the system. There are few applications related to reliability analysis using PINN includes [22-23].

In this study, a 16-storey steel moment resisting (MR) frame coupled with a self-centering damper is considered to estimate the design parameters of the damper using RBDO so that the proposed system can show the effective performance when subjected to a future seismic event. In general, the MR frame is designed in such a way that earthquake-induced vibration is mitigated through the inelastic deformation of the structural members. As a consequence, large residual deformation is often seen, which leads to damage in structural members [24]. Self-centering dampers are one of the alternatives that can reduce the residual deformation of the structural system susceptible to seismic loads. There have been numerous self-centering devices reported in the literature, such as post-tensioned braces [25], shape memory alloy [26], ring springs [27], etc. Among these, viscous dampers have been widely used in self-centering systems to reduce earthquake-induced vibration [28]. By combining a flag-shaped system with various energy dissipation components, such as hysteretic, viscous, and viscoelasto-plastic connected in series or parallel, Kam et al. [28] proposed various self-centering systems. The performance of the proposed controllers was established under an ensemble of far-field and near-field ground motions. Dong et al. [29] studied the inelastic response spectra of the self-centering structure with the flag-shaped hysteretic response under near-fault pulse-type ground motions. Kitayama and Constantinou [30] evaluated the building's residual drift and probabilistic collapse resistance using fluidic self-centering devices.

Since the self-centering viscous (SC-VD) damper is a passive device, it is necessary to optimize the design of passive devices under uncertainty to guarantee the controller will function satisfactorily for the duration of its service life. Therefore, the RBDO method is used in this study to estimate the optimal parameters related to the hysteresis of SC-VD. The probability of failure of the structural system is estimated using the PDF of the limit state function, which is evaluated using a PINN-based PDEM framework. In light of this, the current work sets the following objectives in order to evaluate the reliability-based design of the SC-VD in the presence of uncertainties-

- Using OpenSees, develop a model of a high-rise steel moment-resisting frame coupled with a self-centering viscous damper placed at every floor.

- Develop a physics-informed neural network-based probability density evolution framework for estimating the transition probability density function of the performance function, which is used to calculate the first-passage failure probability of the structure.
- Investigate the proposed control strategy's performance range in various operational scenarios.

MODELING OF STEEL MR-FRAME WITH SC-VD

In this section, a brief description of force-displacement hysteresis of SC-VD is illustrated. The hysteresis of SC-VD is modeled in OpenSees as a combination of the hysteresis of a self-centering (SC) damper and a viscous damper, as shown in Figure 1. The flag-shaped hysteresis of an SC damper (in Figure 1(a)) is characterized by an initial stiffness, k_1 , a post-activation stiffness, k_2 , activation force, F_0 and an energy dissipation factor, β . The parameter β is the ratio of forward to reverse activation force. Similarly, the force-displacement hysteresis of the viscous damper (in Figure 1(b)) is expressed in the following form:

$$F = C_d |\dot{u}|^{\alpha_d} \text{sgn}(\dot{u}) \quad (1)$$

where the force offered by the viscous damper and the displacement of the damper are denoted by F and u , respectively. In Eq. (1), C_d and α_d are the damping coefficient and damping exponent, respectively. The signum function is denoted by $\text{sgn}(\cdot)$, as in Eq. (1). In this study, a parallel connection between a viscous damper and a SC damper is used to assess the hysteresis response of the SC-VD.

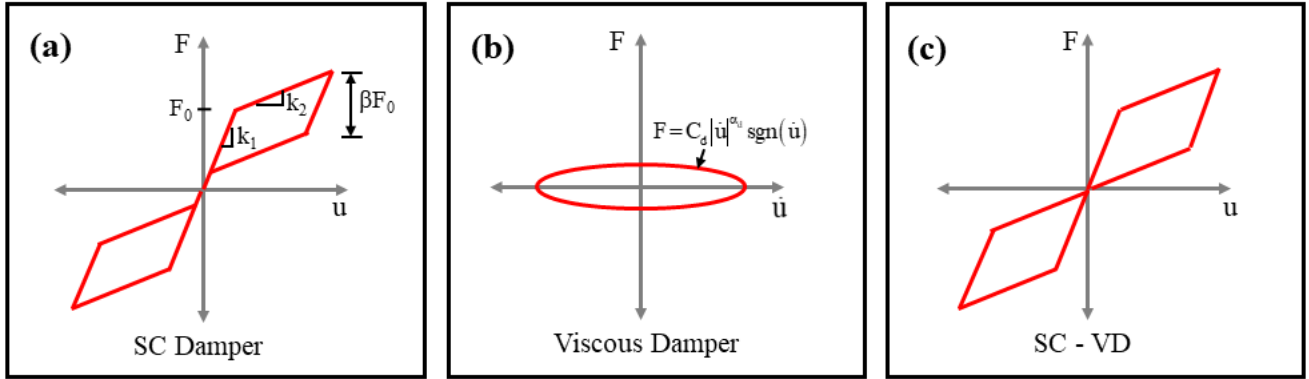


Figure 1. Force - displacement hysteresis of (a) SC damper; (b) Viscous damper and (c) SC-VD.

In this study, a 16-storey steel moment-resistant (MR) frame with a self-centering viscous damper is modelled using the open-source finite element modeling software OpenSees (Open System for Earthquake Engineering Simulation), shown in Figure 2. With a span length of 8 m, the building has three bays. Except for the first storey, whose height is 4.5 m above the ground, the building's storey height is 4 m. At roof level, the dead and live loads are assumed to be 1.68 kPa and 0.96 kPa, respectively. The weight of the cladding is 1.2 kPa, while the weights for the floor levels are respectively 3.35 kPa and 1.68 kPa. The steel MRF is modeled using the *Hardening Material* model from the OpenSees material library. The steel members' material parameters include a Young's modulus of 206 GPa, a yield strength of 345 MPa, a Poisson's ratio of 0.3, an isotropic hardening modulus of zero, and a kinematic hardening modulus of 1000 MPa. The beams and columns of the steel MRF are assumed to be wide-flange steel sections, whose cross-sectional properties are tabulated in Table 1. The beams and columns of the steel MR frame are modeled using the *NonlinearBeamColumn* element with *Uniaxial Material Hardening* model. Leaning columns with gravity loads are attached to the frame with truss elements in order to capture P-Delta effects. In Figure 2, it is shown that at every floor, self-centering viscous dampers are arranged diagonally. In OpenSees, a *Two-node Link element* is used, and two *Uniaxial Materials* - namely, *SelfCentering Material* and *Viscous Material* - are combined in parallel. The *SelfCentering Material* is characterized by four parameters, i.e., k_1 , k_2 , F_0 , and β and the viscous damper is modeled by *Viscous Material* model in the OpenSees material library, which has two parameters, i.e., C_d and α_d , as shown in Figure 1.

Table 1. The cross-section properties of beam and column of 16-storey steel MR frame

Property	Storey 1-4		Storey 5-8		Storey 9-12		Storey 13-16	
	Beam	Column	Beam	Column	Beam	Column	Beam	Column
d (mm)	607.6	407.4	612.2	393.2	544.3	375.4	463.3	363.7
b _f (mm)	228.3	403.6	229.1	399.1	212.2	393.7	191.9	371.0
t _f (mm)	17.3	43.7	19.6	36.6	21.2	27.7	17.7	21.9
t _w (mm)	11.2	27.2	11.9	22.6	13.1	17.3	10.6	13.4
nf _{dw}	27	15	27	16	27	15	21	14
nf _{tw}	2	2	2	2	2	2	2	2
nf _{bf}	10	15	10	16	10	15	9	14
nf _{tf}	2	4	2	4	2	4	2	4

d: Section depth; b_f: Flange width; t_f: Flange thickness; t_w: Web thickness; nf_{dw}: Number of fibers along web depth; nf_{tw}: Number of fibers along web thickness; nf_{bf}: Number of fibers along flange width; nf_{tf}: Number of fibers along flange thickness.

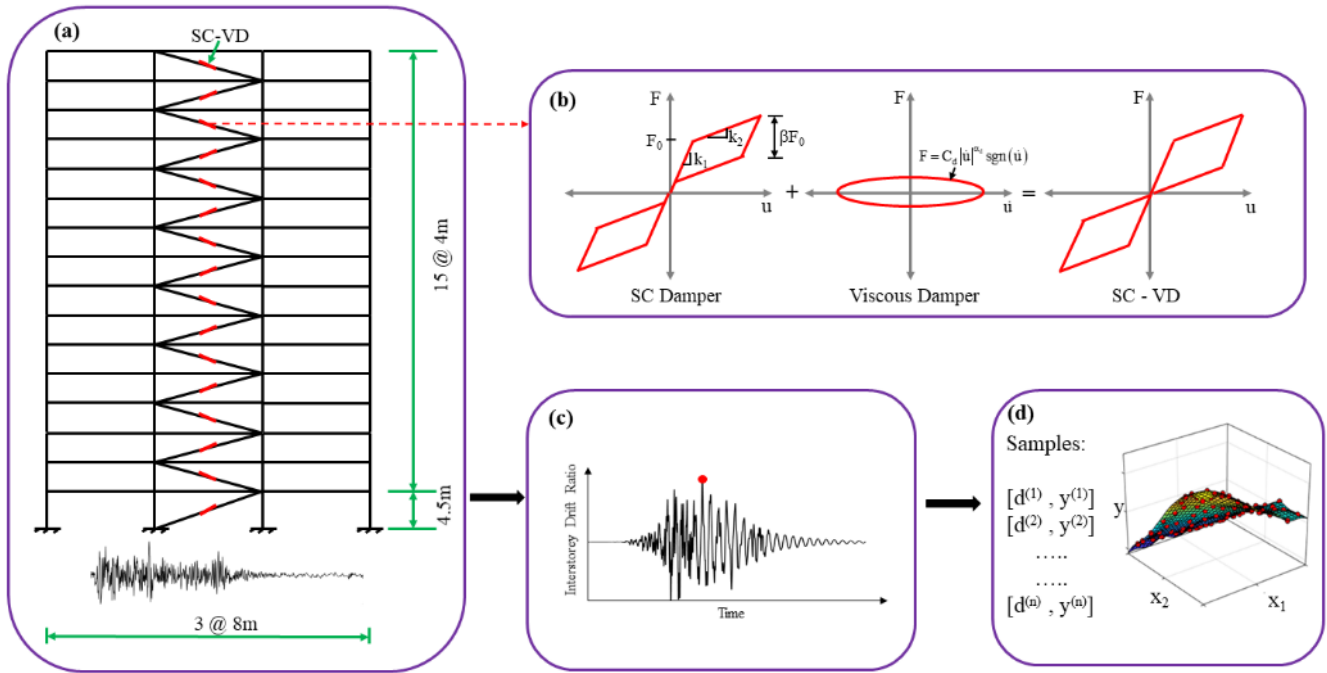


Figure 2. (a) Layout of 16-storey steel moment resisting frame with SC-VD; (b) Force - Displacement hysteresis of SC-VD; (c) Performance function and (d) Response surface of limit state function using PINN.

FIRST-PASSAGE PROBABILITY ESTIMATION USING PDEM

The probability density evolution method (PDEM), developed based on the principle of probability conservation, was proposed by Li and Chen [16] and is used in this study to estimate the PDF of a stochastic process. Assume that Y represents a system's state and that t is the parameter describing how that state evolves. The system's state shifts from $Y(t)$ to $Y(t + dt)$ during dt , the time step. On the other hand, it is assumed that the system's state at time t , $Y(t)$, is a part of a region, which is indicated by Ω_t . The state $Y(t + dt)$ corresponds to the area Ω_{t+dt} at the time $(t+dt)$. Additionally, it is assumed that the state $Y(t)$ is a function of a set of random variables, Θ and that it remains unchanged for the duration of the stochastic process. The joint probability space by Y and Θ is then expressed as follows in accordance with the probability conservation principle.

$$\Pr\{[Y(t + dt), \Theta] \in \Omega_{t+dt} \times \Omega_{\Theta}\} = \Pr\{[Y(t), \Theta] \in \Omega_t \times \Omega_{\Theta}\} \quad (2)$$

where the domain of the random variables is denoted by Ω_{Θ} . Eq. (2) can be used to formulate the generalized density evolution equation (GDEE) in the PDEM, which is given by

$$\frac{\partial p_{Y\Theta}(y, \theta, t)}{\partial t} + \dot{Y}(\theta, t) \frac{\partial p_{Y\Theta}(y, \theta, t)}{\partial y} = 0 \quad (3)$$

The initial condition of the above partial differential equation is expressed as

$$p_{Y\Theta}(y, \theta, t)|_{t=0} = \delta[y - Y(\theta, 0)] p_{\Theta}(\theta) \quad (4)$$

where $p_{\Theta}(\theta)$ is the joint PDF of the random variables, Θ and $\delta(\cdot)$ denotes the Dirac delta function. The joint PDF between Y and Θ , i.e., $p_{Y\Theta}(y, \theta, t)$ is estimated by solving Eq. (3) and Eq. (4) using physics-informed neural network, which is discussed in the following section. The PDF of Y , i.e., $p_Y(y, t)$ is computed by integrating over region Θ which is given by

$$p_Y(y, t) = \int_{\Omega_{\Theta}} p_{Y\Theta}(y, \theta, t) d\theta \quad (5)$$

This study considers the first-passage failure problem, in which the likelihood that a system will fail is expressed as

$$P_f = \Pr\{Y(t) \in \Omega_f, \exists t \in [0, T]\} \quad (6)$$

where $\Pr\{\cdot\}$ denotes the probability operator, Ω_f is the failure domain of $Y(t)$ and the duration of time is represented by $[0, T]$. Using the principle of an equivalent extreme-value event, Eq. (6) can be reformulated as follows

$$P_f = \Pr\{Y_{\text{EEV}} \in \Omega_f, \exists t \in [0, T]\} \quad (7)$$

where Y_{EEV} is the equivalent extreme value (EEV) of $Y(t)$ within the duration $[0, T]$ [31]. The probability of failure of the system can be estimated by integrating over the failure domain, is given by

$$P_f = \Pr\{Y_{\text{EEV}} \geq Y_{\text{Thres}}\} = \int_{Y_{\text{Thres}}}^{\infty} p_{Y_{\text{EEV}}}(y) dy \quad (8)$$

where $p_{Y_{\text{EEV}}}$ denotes the PDF of EEV of $Y(t)$ and the threshold value of the system is represented by Y_{Thres} . It can be seen from Eq. (8) that Y_{EEV} is not time dependent function. Therefore, Eq. (3) cannot be used directly to estimate PDF of Y_{EEV} . To make Y_{EEV} into time dependent function, a virtual stochastic process is assumed which is given by

$$\mathcal{V}(\tau) = Y_{\text{EEV}} \sin(\omega\tau); \quad \tau \in [0, 1] \quad (9)$$

where $\omega = 5\pi/2$. It is seen from Eq. (9) that $\mathcal{V}(\tau)|_{\tau=0} = 0$ and $\mathcal{V}(\tau)|_{\tau=1} = Y_{\text{EEV}}$. Therefore, GDEE in Eq. (3) can be used to estimate PDF of $\mathcal{V}(\tau)$ which is given by

$$\frac{\partial p_{\mathcal{V}\Theta}(v, \theta, \tau)}{\partial \tau} + \dot{\mathcal{V}}(\theta, \tau) \frac{\partial p_{\mathcal{V}\Theta}(v, \theta, \tau)}{\partial v} = 0; \quad p_{\mathcal{V}\Theta}(v, \theta, \tau)|_{\tau=0} = \delta(v) p_{\Theta}(\theta) \quad (10)$$

$$p_{\mathcal{V}}(v, \tau) = \int_{\Omega_{\Theta}} p_{\mathcal{V}\Theta}(v, \theta, \tau) d\theta \quad (11)$$

Once the PDF of $\mathcal{V}(\tau)$ is estimated, $p_{Y_{\text{EEV}}}$ is estimated by substituting τ equals to 1 into $p_{\mathcal{V}}(v, \tau)$, is expressed as follows

$$p_{Y_{\text{EEV}}}(y) = p_{\mathcal{V}}(v, \tau)|_{v=y, \tau=1} \quad (12)$$

PHYSICS-INFORMED NEURAL NETWORK

Physics-informed neural network (PINN), a class of feed-forward neural network, is one in which the network is subject to physical restrictions in the form of a loss function [21]. The PINN has the same architecture as any other feed-forward neural network, and its output is expressed as a nested nonlinear transformation of data from the network's hidden layers. Consider a nonlinear partial differential equation whose expression can be written as follows

$$\frac{\partial p(y,t)}{\partial t} + \mathcal{N}[p(y,t); \chi] = 0; \quad p(y,t) = \mathcal{G}(y,t); \quad p(y,0) = \mathcal{H}(y) \quad (13)$$

where $p(y,t)$ is a function of spatial variable, y and temporal variable, t , is the solution of Eq. (13) which is estimated using PINN. In the above equation, $\mathcal{N}[p(y,t); \chi]$ is the nonlinear differential operator and χ is the coefficient of the differential operator. Also, the boundary and initial conditions of the above partial differential equation are denoted by $\mathcal{G}(y,t)$ and $\mathcal{H}(y)$, respectively. To train the PINN, an N number of collocation points, i.e., $\{y^i, t^i\}_{i=1}^N$ are generated from the domain $y \in \Omega, t \in \mathcal{T}$. To estimate the derivative of $p(y,t)$ with respect to y and t at every collocation points, automatic differentiation is used. Therefore, loss functions including initial conditions and boundary conditions, as in Eq. (13) are evaluated using the obtained values of $p(y,t)$ and its derivatives at every collocation points. Once the loss functions are evaluated, a weighted sum of loss function is constructed which is to be minimized with the aim of minimal of difference between actual and predicted values of $p(y,t)$. If the predicted values of $p(y,t)$ converge with the actual values, i.e., the value of the weighted loss function is less than a specified tolerance, the algorithm is terminated; otherwise, update the weight and bias parameters of the neural network by minimizing weighted loss function using stochastic gradient descent method. The process continues until convergence is achieved. A schematic diagram of PINN is shown in Figure 3.

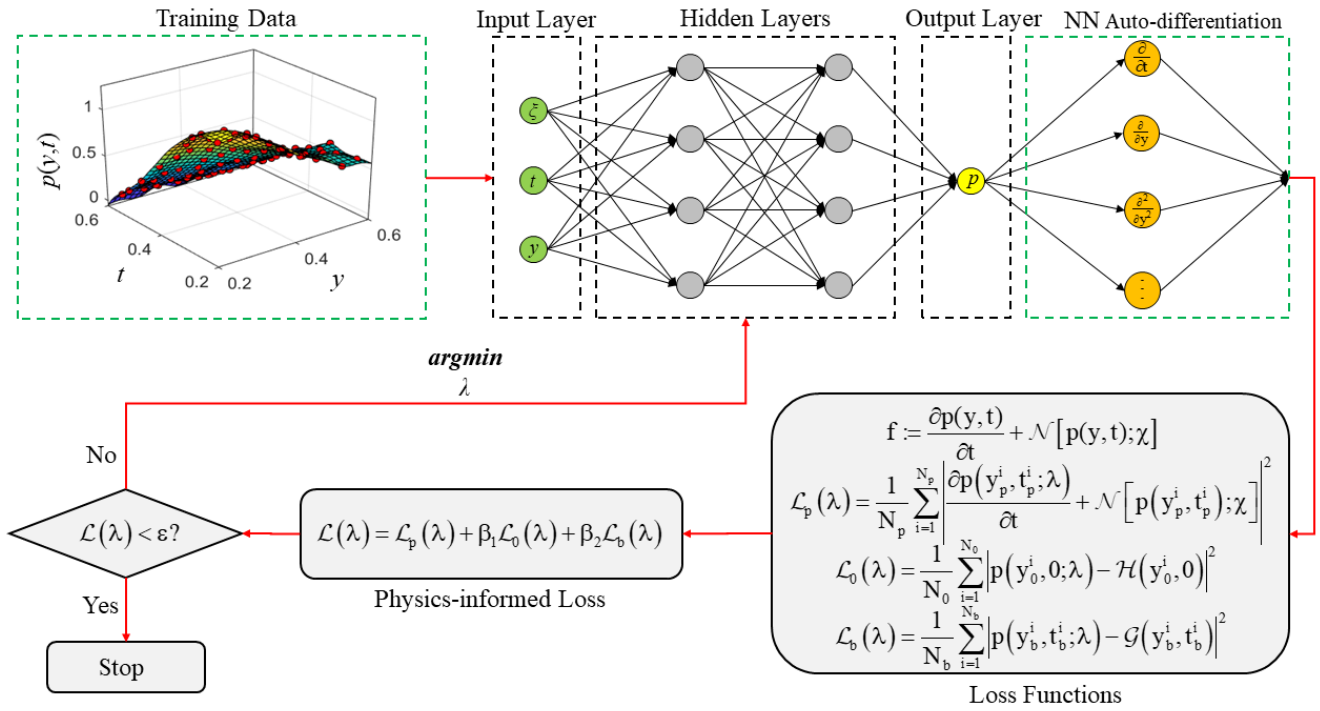


Figure 3. Schematic diagram of physics-informed neural network.

The loss function corresponding to Eq. (13) can be constructed in the following form:

$$\mathcal{L}_p(\lambda) = \frac{1}{N_p} \sum_{i=1}^{N_p} \left| \frac{\partial p(y_p^i, t_p^i; \lambda)}{\partial t} + \mathcal{N}[p(y_p^i, t_p^i; \lambda); \chi] \right|^2; \quad \mathcal{L}_0(\lambda) = \frac{1}{N_0} \sum_{i=1}^{N_0} |p(y_0^i, 0; \lambda) - \mathcal{H}(y_0^i, 0)|^2 \quad (14)$$

$$\mathcal{L}_b(\lambda) = \frac{1}{N_b} \sum_{i=1}^{N_b} |p(y_b^i, t_b^i; \lambda) - \mathcal{G}(y_b^i, t_b^i)|^2 \quad (15)$$

To train the neural network, a weighted sum of the above loss functions is considered which is expressed as follows

$$\mathcal{L}(\lambda) = \mathcal{L}_p(\lambda) + \beta_1 \mathcal{L}_0(\lambda) + \beta_2 \mathcal{L}_b(\lambda) \quad (16)$$

where β_1 and β_2 are the weight parameters to adjust the relative importance of each residual term. To estimate the proper weight and bias parameters of the neural network, the weighted loss function in Eq. (16) is minimized so that the

predicted value, $p(y,t)$ from the PINN and the actual value, $p(y,t)$ from the model evaluation converge. In this study, the stochastic gradient descent algorithm is used to estimate the weight and bias components of the neural network.

RELIABILITY-BASED DESIGN OPTIMIZATION OF SC-VD

In this study, PINN-based PDEM framework is adopted to compute the failure probability which is utilized for reliability-based design optimization of self-centering viscous damper (SC-VD). When the system operates in a stochastic environment, the SC-VD with deterministic design provides unreliable performance. In order to ensure that the controller performs satisfactorily during anticipated future seismic occurrences, it must be designed (i.e., SC-VD related parameters must be tuned). For this purpose, maximum inter-storey drift ratio among all floors is assumed as an objective function to measure the efficiency of the controller. The probability of failure for this system is constructed as follows

$$P_f = \Pr \left\{ \max_{k \in \{1, N_F\}} (\text{IDR}_k) - \text{IDR}_{\max} \geq 0 \right\} \quad (17)$$

where IDR_k is the maximum inter-storey drift ratio of k^{th} floor where total number of floor is denoted by N_F . Also, IDR_{\max} is the maximum allowable inter-storey drift ratio which equals to 2.5% according to NBC 2015. Here, the uncertainty is considered to be associated with the ground motion only. For a set of tuning parameters (which is random) of SC-VD, the maximum inter-storey drift ratio among all floors is estimated for every ground motion. Once it is estimated for all ground motion corresponding to a set of tuning parameters, the PDF of IDR is estimated using PINN-based PDEM framework in which the loss function of the neural network is formed using Eq. (10) and Eq. (11), is given by

$$\mathcal{L}(\lambda) = \frac{1}{N_p} \sum_{i=1}^{N_p} \left| \frac{\partial p_{v\theta}(\mathbf{v}_p^i, \theta, \tau_p^i; \lambda)}{\partial \tau} + \dot{v}(\theta, \tau_p^i) \frac{\partial p_{v\theta}(\mathbf{v}_p^i, \theta, \tau_p^i; \lambda)}{\partial v} \right|^2 + \beta_1 \left\{ \frac{1}{N_0} \sum_{i=1}^{N_0} \left| p_{v\theta}(\mathbf{v}_0^i, \theta, 0; \lambda) - \delta(v) p_\theta(\theta) \right|^2 \right\} \quad (18)$$

Once the PDF of IDR is estimated using PINN-based PDEM and Eq. (12) for a given set of tuning parameters, the probability of failure is estimated by one-dimensional integration over failure region, is given by

$$P_f = \Pr \left\{ \text{IDR} \geq \text{IDR}_{\max} \right\} = \int_{\text{IDR}_{\max}}^{\infty} p_{\text{IDR}}(\text{IDR}) d\text{IDR} \quad (19)$$

Once the probability of failure is obtained using Eq. (19) for all values of tuning parameters of SC-VD, the RBDO problem is formulated as

$$\mathbf{d}^* = \underset{\mathbf{d}}{\text{argmin}} \left[P_f(\mathbf{d}) \right] \quad \text{s.t.} \quad \mathbf{d}_{\text{ll}} \leq \mathbf{d} \leq \mathbf{d}_{\text{ul}} \quad (20)$$

where \mathbf{d} is the tuning parameters of SC-VD i.e., initial stiffness (k_1), post-activation stiffness (k_2), forward activation force (F_0), and the ratio of forward to reverse activation force (β) of the self-centering material, as well as the damping coefficient (C_d) of viscous material. The lower and upper bound of the design parameters are represented by \mathbf{d}_{ll} and \mathbf{d}_{ul} , respectively.

NUMERICAL RESULTS & DISCUSSION

A 16-storey steel MRF is used in this section to illustrate the reliability-based design optimization for a self-centering viscous damper (SC-VD). The SC-VD tuning parameters include the initial stiffness (k_1), post-activation stiffness (k_2), forward activation force (F_0), the ratio of forward to reverse activation force (β) for the self-centering damper, and the damping coefficient (C_d) for the viscous damper (which is modelled in OpenSees as a combination of self-centering damper and viscous damper) are optimized in the light of ground motion uncertainty. Thus, two types of ensembles of ground acceleration records are considered, i.e., far-field and near-field ground motions, which are taken from the FEMA P695 (ATC-63). The near-field ground motions set includes two types of near-field ground motions, i.e., pulse and non-pulse. These ground motions are recorded within 50 km epicentral distance. A set of 14 ground motions (each having two horizontal components) is considered. The far-field ground motions are selected within a 100 km epicentral distance, and the soil type is classified as type C and type D, according to the NEHRP site classification. To do RBDO, the lower and upper bounds of the tuning parameters of SC-VD are assumed as: $k_1 \sim U [100, 500]$ kN/mm, $k_2 \sim U [2.5, 20]$ kN/mm, $F_0 \sim U [300, 600]$ kN, $\beta \sim U [0.3, 0.6]$ and $C_d \sim U [5, 25]$ kN/(mm/s)^{0.4}, respectively, are assumed to follow the uniform distribution. These bounds of the tuning parameters are kept constant.

With this in view, the probability of failure of the structure is estimated using a PINN-based PDEM. The first step of the numerical procedure is to use the GF-discrepancy method to create 100 collocation points of random variables. For each ground motion, the system's response is evaluated. The inter-storey drift ratio is chosen as the extreme event. Once the extreme event

is computed for all collocation points, the PDF of Y_{EEV} is estimated using PDEM, as defined in Eq. (10), Eq. (11) and Eq. (12). The partial differential equation in Eq. (10) subjected to initial condition depicted in Eq. (11) is solved using PINN. The architecture of the neural network is set to 8 hidden layers with 30 neurons in each hidden layer. The hyperbolic tangent function is used as an activation function. The Adam optimization algorithm is used to compute the weight and bias of the network, in which the learning rate is assumed to be 0.001. For every set of tuning parameters, the PDF of inter-storey drift ratio is estimated based on PINN-based PDEM framework. Figure 4(a) and Figure 5(a) show the PDF of maximum inter-storey drift ratio among all floors for far-field and near-field ground motion, respectively. For validation purpose, the Monte-Carlo simulation is adopted to find the PDF. It is seen from Figure 4(a) and Figure 5(a), the PDF estimated using proposed framework is well matched with Monte Carlo simulation. Using this PDF, the probability of failure is estimated by performing one-dimensional integration over failure domain, as in Eq. (8) in which the maximum inter-storey drift ratio is taken as 2.5%. Once the probability of failure is estimated for all set of tuning parameters of SC-VD, the RBDO is performed on the surface which are shown in Figure 4(b) and Figure 5(b) for far-field and near-field ground motions, respectively. The optimal tuning parameters are estimated at the point on the response surface where the probability of failure is minimum. The optimal tuning parameters of SC-VD are tabulated in Table 2.

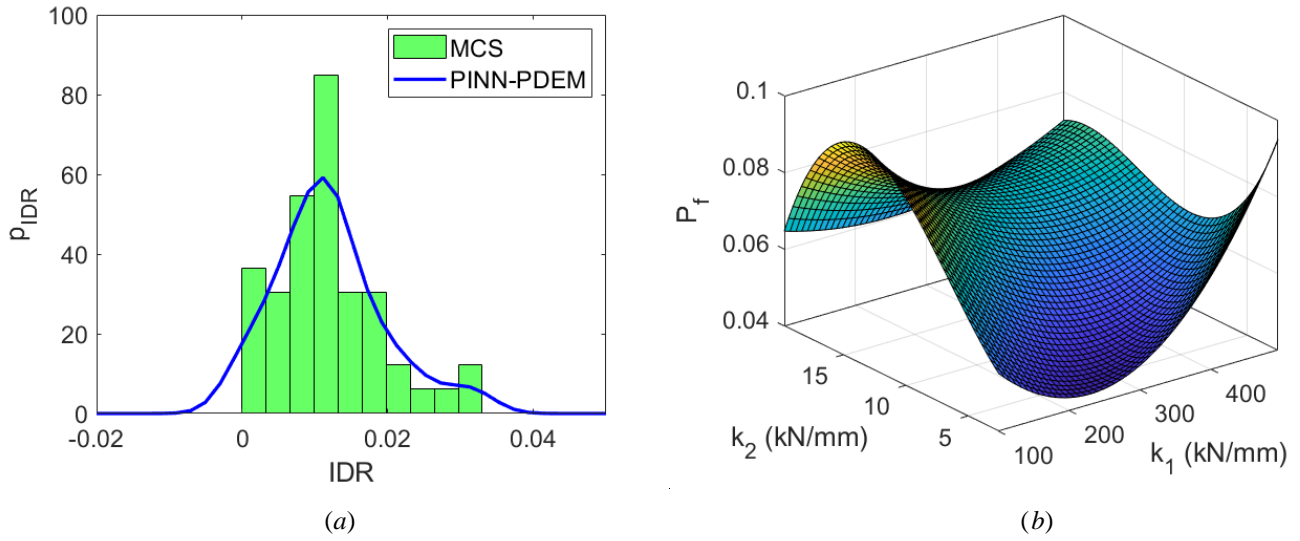


Figure 4. (a) PDF of maximum inter-storey drift ratio and (b) response surface of probability of failure for far-field ground motion

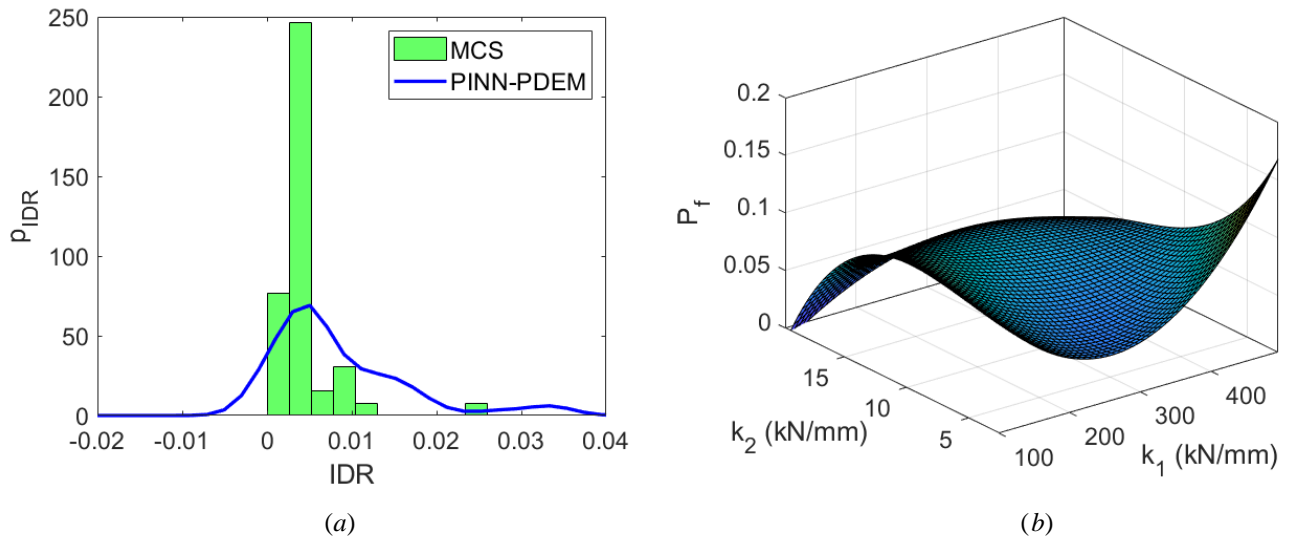


Figure 5. (a) PDF of maximum inter-storey drift ratio and (b) response surface of probability of failure for near-field ground motion

Table 2. Tuning parameters of SC-VD for far-field and near-field ground motions

Parameters	Storey 1-2		Storey 3-6		Storey 7-10		Storey 11-13		Storey 14-16	
	Far	Near	Far	Near	Far	Near	Far	Near	Far	Near
k_1	162.5	143.7	262.5	381.2	437.5	156.2	187.5	331.2	362.5	381.2
k_2	5.2	14.8	12.9	6.1	3.1	3.9	5.2	3.3	14.9	15.3
F_0	459.4	351.5	178.1	217.2	240.6	185.9	396.9	420.3	115.6	170.3
β	0.55	0.53	0.59	0.38	0.48	0.52	0.33	0.38	0.36	0.36
C_d	21.9	15.3	14.4	19.7	24.3	10.9	18.1	15.3	6.8	7.2

With these optimal tuning parameters, the top floor displacement of the steel MR frame is evaluated which is shown in Figure 6(a) and Figure 6(b) for far-field and near-field ground motions, respectively. Similarly, the corresponding maximum residual drift at all floors is depicted in Figure 7(a) and Figure 7(b) for far-field and near-field ground motions, respectively.

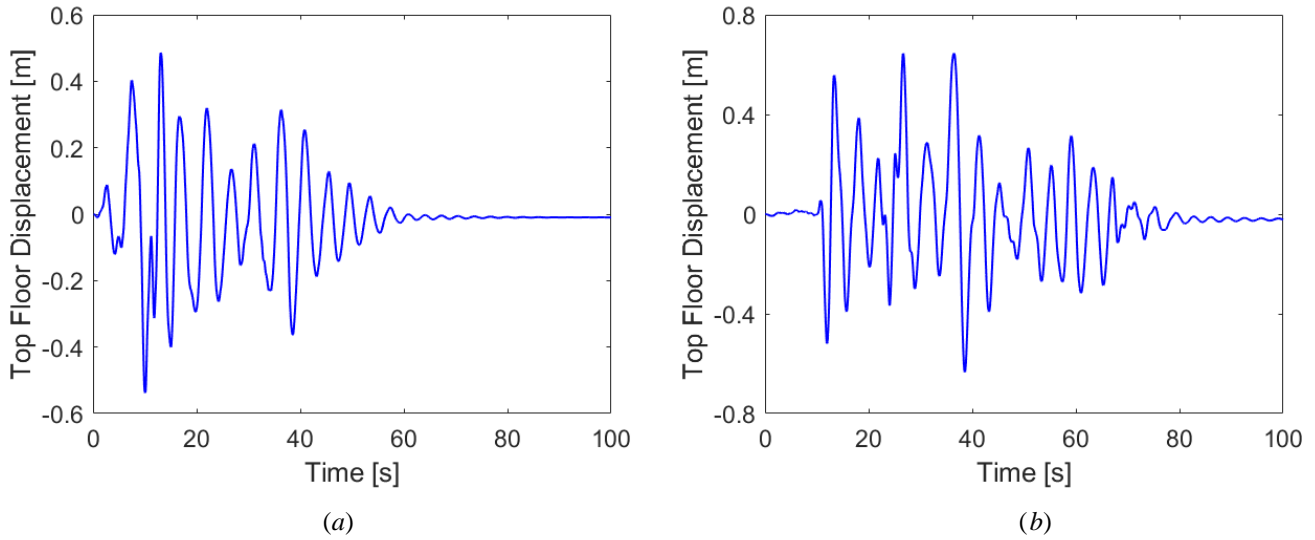


Figure 6. Top floor displacement for (a) far-field and (b) near-field ground motions

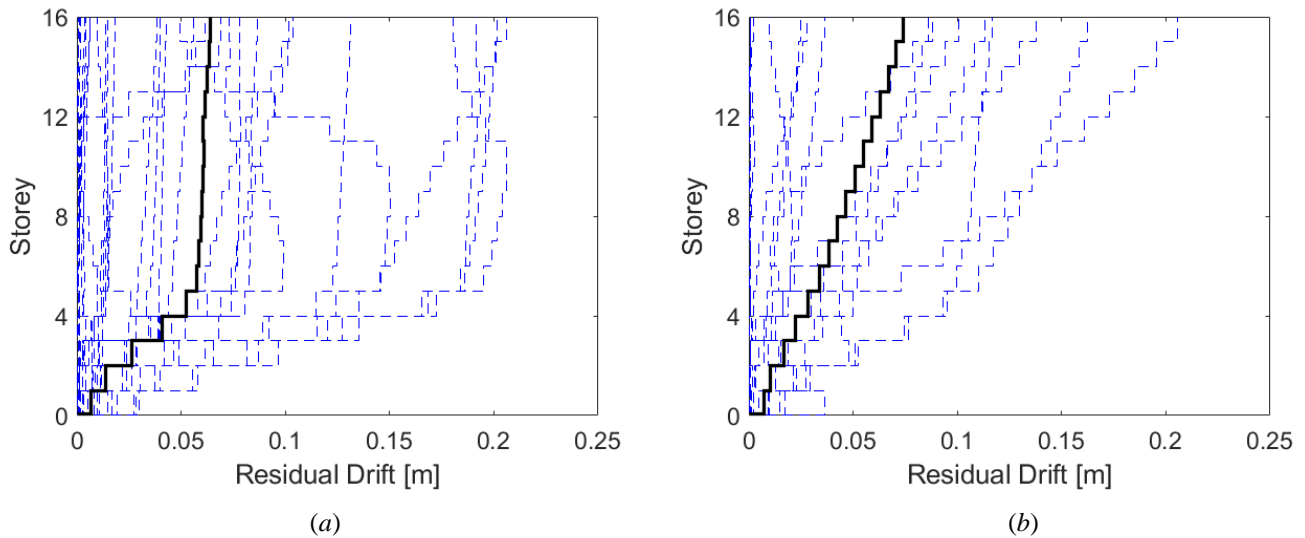


Figure 7. Maximum residual drift at floor level for (a) far-field and (b) near-field ground motions

CONCLUSIONS

This study proposed fine-tuning the self-centering viscous damper for reliable performance in the presence of ground motions. A steel moment-resisting structure has dampers installed on each floor, acting as a brace. In order for the proposed damper to operate satisfactorily against any future earthquakes, this study aims to fine-tune its stiffness and damping properties under ground motion uncertainty. A physics-informed neural network-based probability density evolution method is used to design the phenomenological parameters of the self-centering viscous damper. Two different ensembles of ground motions (i.e., far-field and near-field) are used to establish the performance of the proposed damper. The major observations from this study are reported below:

- The accuracy of the proposed framework is validated with the Monte Carlo simulation. It is seen from the numerical investigation that the solution using the proposed framework is consistent with the Monte Carlo simulation.
- It is seen from the numerical analysis that 100 collocation samples of the tuning parameters of SC-VD are required to get the satisfactory performance of PINN, which leads to a reduced computational cost compared to any numerical method such as the finite difference method.

ACKNOWLEDGMENTS

This study was funded by Natural Sciences and Engineering Research Council of Canada under the Discovery Grant programs (RGPIN-2019- 05584) and BC Forestry Innovation Investment's (FII) Wood First Program.

REFERENCES

- [1] Shinozuka, M. (1972). "Monte Carlo solution of structural dynamics". *Computers & Structures*, 2(5-6), 855-874.
- [2] Au, S.K. and Beck, J.L. (2001). "Estimation of small failure probabilities in high dimensions by subset simulation". *Probabilistic Engineering Mechanics*, 16(4), 263-277.
- [3] Engelund, S. and Rackwitz, R. (1993). "A benchmark study on importance sampling techniques in structural reliability". *Structural Safety*, 12(4), 255-276.
- [4] Gaspar, B., Teixeira, A.P. and Soares, C.G. (2014). "Assessment of the efficiency of Kriging surrogate models for structural reliability analysis". *Probabilistic Engineering Mechanics*, 37, 24-34.
- [5] Marelli, S. and Sudret, B. (2018). "An active-learning algorithm that combines sparse polynomial chaos expansions and bootstrap for structural reliability analysis". *Structural Safety*, 75, 67-74.
- [6] Bourinet, J.M., Deheeger, F. and Lemaire, M. (2011). "Assessing small failure probabilities by combined subset simulation and support vector machines". *Structural Safety*, 33(6), 343-353.
- [7] Chojaczyk, A.A., Teixeira, A.P., Neves, L.C., Cardoso, J.B. and Soares, C.G. (2015). "Review and application of Artificial Neural Networks models in reliability analysis of steel structures". *Structural Safety*, 52, 78-89.
- [8] Zhao, Y.G. and Lu, Z.H. (2007). "Fourth-moment standardization for structural reliability assessment". *Journal of Structural Engineering*, 133(7), 916-924.
- [9] Novi Inverardi, P.L. and Tagliani, A. (2003). "Maximum entropy density estimation from fractional moments". *Communications in Statistics-Theory and Methods*, 32(2), 327-345.
- [10] Liu, J., Hu, Y., Xu, C., Jiang, C. and Han, X. (2016). "Probability assessments of identified parameters for stochastic structures using point estimation method". *Reliability Engineering & System Safety*, 156, 51-58.
- [11] Xu, J. and Lu, Z. H. (2017). "Evaluation of moments of performance functions based on efficient cubature formulation". *Journal of Engineering Mechanics*, 143(8), 06017007.
- [12] Frank, T. D. (2005). "*Nonlinear Fokker-Planck Equations: Fundamentals and Applications*". Springer Science & Business Media.
- [13] Crandall, S. H. (1963). "Perturbation techniques for random vibration of nonlinear systems". *The Journal of the Acoustical Society of America*, 35(11), 1700-1705.
- [14] Khas' minskii, R. Z. (1966). "A limit theorem for the solutions of differential equations with random right-hand sides". *Theory of Probability & Its Applications*, 11(3), 390-406.
- [15] Wu, W.F. and Lin, Y.K. (1984). "Cumulant-neglect closure for non-linear oscillators under random parametric and external excitations". *International Journal of Non-Linear Mechanics*, 19(4), 349-362.
- [16] Li, J. and Chen, J. (2008). "The principle of preservation of probability and the generalized density evolution equation". *Structural Safety*, 30(1), 65-77.
- [17] Xu, J. and Feng, D. C. (2019). "Stochastic dynamic response analysis and reliability assessment of non-linear structures under fully non-stationary ground motions". *Structural Safety*, 79, 94-106.
- [18] Wan, Z., Chen, J., Li, J. and Ang, A.H.S. (2020). "An efficient new PDEM-COM based approach for time-variant reliability assessment of structures with monotonically deteriorating materials". *Structural Safety*, 82, 101878.

- [19] Xu, J., Xu, S. and Yuan, Z. (2020). "Probabilistic seismic analysis of single-layer reticulated shell structures controlled by viscoelastic dampers with an effective placement". *Engineering Structures*, 222, 111052.
- [20] Chen, J., Yang, J. and Li, J. (2016). "A GF-discrepancy for point selection in stochastic seismic response analysis of structures with uncertain parameters". *Structural Safety*, 59, 20-31.
- [21] Raissi, M. and Karniadakis, G.E. (2018). "Hidden physics models: Machine learning of nonlinear partial differential equations". *Journal of Computational Physics*, 357, 125-141.
- [22] Zhang, C. and Shafieezadeh, A. (2022). "Simulation-free reliability analysis with active learning and Physics-Informed Neural Network". *Reliability Engineering & System Safety*, 226, 108716.
- [23] Zhou, T., Zhang, X., Droguett, E. L. and Mosleh, A. (2023). "A generic physics-informed neural network-based framework for reliability assessment of multi-state systems". *Reliability Engineering & System Safety*, 229, 108835.
- [24] McCormick, J., DesRoches, R., Fugazza, D. and Auricchio, F. (2007). "Seismic assessment of concentrically braced steel frames with shape memory alloy braces". *Journal of Structural Engineering*, 133(6), 862-870.
- [25] Chou, C.C. and Chen, Y.C. (2015). "Development of steel dual-core self-centering braces: Quasi-static cyclic tests and finite element analyses". *Earthquake Spectra*, 31(1), 247-272.
- [26] Chang, Z., Xing, G., Han, M. and Liu, B. (2022). "Multiparameter optimization design of self-centering friction damper using shape memory alloy bars". *Journal of Earthquake Engineering*, 1-19.
- [27] Filiatrault, A., Tremblay, R. and Kar, R. (2000). "Performance evaluation of friction spring seismic damper". *Journal of Structural Engineering*, 126(4), 491-499.
- [28] Kam, W.Y., Pampanin, S., Palermo, A. and Carr, A.J. (2010). "Self-centering structural systems with combination of hysteretic and viscous energy dissipations". *Earthquake Engineering & Structural Dynamics*, 39(10), 1083-1108.
- [29] Dong, H., Han, Q., Du, X., Cheng, S. and He, H. (2021). "Inelastic response spectra of self-centering structures with the flag-shaped hysteretic response subjected to near-fault pulse-type ground motions". *Earthquake Spectra*, 37(4), 2767-2794.
- [30] Kitayama, S. and Constantinou, M.C. (2016). "Probabilistic collapse resistance and residual drift assessment of buildings with fluidic self-centering systems". *Earthquake Engineering & Structural Dynamics*, 45(12), 1935-1953.
- [31] Das, S. and Tesfamariam, S. (2023). "Reliability analysis of structures using probability density evolution method and stochastic spectral embedding surrogate model". *Earthquake Engineering & Structural Dynamics*.